

Neuroprotective Effect of Dichloromethane Extraction From *Piper nigrum* L. and *Piper longum* L. on Permanent Focal Cerebral Ischemia Injury in Rats

Shiyao Hua, MS,^{*,#} Bing Wang, MS,^{*,#} Rong Chen, MS,^{*,#} Yuanbin Zhang, MS,^{||} Yiwei Zhang, MS,[§] Tingting Li, MS,[¶] Lin Dong, PhD,^{*,†,‡} and Xueyan Fu, PhD^{*,†,‡}

Background: *Piper nigrum* L. and *Piper longum* L. consist a classic formula in traditional Chinese Hui medicine and are widely used in treatment of stroke. To examine the therapeutic effect of neuron injury after apoplexy, we used a permanent middle cerebral artery occlusion model in rats to investigate the effects of dichloromethane fraction (DF) of *Piper nigrum* L. and *Piper longum* L. **Materials and Methods:** After subjecting the rats to permanent middle cerebral artery occlusion, DF (100 and 200 mg/kg) were administered for 14 days. Neurological deficits and the degree of cerebral tissue injury was detected by 2,3,5-Triphenyltetrazolium Chloride Staining Hematoxylin and eosin staining and Nissl staining. Postsynaptic density protein 95 (PSD-95), synapsin-I (syn-I), and α -synuclein (α -syn) were stained by immunohistochemistry. PSD-95, Ca²⁺/calmodulin (CaM)-dependent protein kinase II (CaMK II), phosphorylated CaMK II (p-CaMK II), CaM, N-methyl D-aspartate receptor subtype 2B (NR2B) expression were detected by Western blot. Meanwhile, phytochemical profile of DF was determined through ultrahigh-performance liquid chromatography-quadrupole time-of-flight mass spectrometry (UPLC-Q-TOF/MS). **Results:** DF alleviated neurological deficits and markedly prevented ischemia-induced cellular damage. Immunohistochemical micrographs revealed that PSD-95 and syn-I proteins increased, and α -syn presented reduced expression in brain samples from the sham group. Western blot analyses revealed that the model group exhibited a noticeable reduction in PSD-95, p-CaMK II, CaM, and NR2B. The DF-treated model group exhibited increased PSD-95, p-CaMK II, CaM, and NR2B. UPLC-Q-TOF/MS analysis revealed eight main components of DF, of which piperine accounted for the largest proportion.

Key Words: Permanent middle cerebral artery occlusion—neuroprotective effects—motor dysfunction—UPLC-Q-TOF/MS

© 2018 National Stroke Association. Published by Elsevier Inc. All rights reserved.

From the ^{*}School of Pharmacy, Ningxia Medical University, Yinchuan, China; [†]Key Laboratory of Hui Ethnic Medicine Modernization, Ministry of Education, Yinchuan, China; [‡]Ningxia Engineering and Technology Research Center for Modernization of Hui Medicine, Yinchuan, China; [§]School of Basic Medical Sciences, Ningxia Medical University, Yinchuan, China; [¶]School of Traditional Chinese Medicine, Ningxia Medical University, Yinchuan, China; and ^{||}School of Pharmacy, Nanjing University of Chinese Medical, Nanjing, China.

Received July 1, 2018; revision received September 29, 2018; accepted November 11, 2018.

Grant support: This work was supported from the National Nature Science Foundation of China by grants (Project No. 81360666 and No. 81860754) and the Foundation of Ningxia Medical University (Project No. 2017023).

Address correspondence to Xueyan Fu, PhD, School of Pharmacy, Ningxia Medical University, No. 692, Shengli Avenue, Xingqing District, Yinchuan 750004, PR China. E-mail: xueyanfu2661@163.com.

[#]Shiyao Hua, Bing Wang, and Rong Chen are co-first authors in this article.

1052-3057/\$ - see front matter

© 2018 National Stroke Association. Published by Elsevier Inc. All rights reserved.

<https://doi.org/10.1016/j.jstrokecerebrovasdis.2018.11.018>

Introduction

Ischemic brain injury produced by stroke or cardiac arrest is a major cause of human neurological disability. During the past decade there has been a small decline, but the burden of stroke remains enormous. Cerebral ischemia can cause serious neuronal damage. From the world wide point of view, stroke is the second leading cause of mortality and disability. In China, stroke was the first leading cause of mortality and morbidity.^{1,2} Stroke is a prominent public health concern but remains a not completely solved issue. In the nervous system, the signals between cells and cells are transmitted by synaptic structure. They are the functional units of neurotransmitters and receptors. The integrity of synaptic structure is the material basis for the normal functioning of neurons.³

The classic formulas consist of *Piper nigrum* L. and *P. longum* L. are widely used in stroke treatment of Hui nationality in traditional Chinese medicine. *Piper nigrum* L. and *P. longum* L. belong to family Piperaceae and are widely cultivated in China and Southeast Asia. These plants are commonly used as household spices (such as food additives and condiments) and traditional medicine by people worldwide, specifically in China and Southeast Asia.⁴ These medicines possess well-documented properties, such as antiplatelet aggregation, antiatherogenic, anti-inflammatory, and antioxidant activities.^{4,5} Our previous studies showed that residues of these plants (extracted by supercritical fluid CO₂) contain ethanol extracts, including supercritical fluid CO₂ extract of *Piper nigrum* L. and *P. longum* L., which cause less irritation, anti-inflammatory in pMCAO in rats.⁶ Cerebral ischemia can lead to structural changes and functional impairment of synaptic neurons which plays an important role in learning and memory. But now, the research on the role of synaptic damage after stroke is not yet mature.

This experiment studied the protective effect of DF on synaptic neurons in pMCAO rats. Chemical composition of DF was simultaneously determined with ultrahigh-performance liquid chromatography-quadrupole time-of-flight mass spectrometry (UPLC-Q-TOF/MS). This study aids in understanding the therapeutic effects of DF neurons on stroke while providing potential strategies for treating ischemic stroke for the development of new drugs from traditional Chinese Medicine.

Materials and Methods

Drugs and Chemicals

The following drugs and chemicals were used: ethanol, methanol, petroleum ether, dichloromethane, and chloral hydrate. The compounds were obtained from Damao Chemical Company (Tianjin, China). DF was suspended in 0.5% (w/v) dimethyl sulfoxide/0.5% (w/v) sodium carboxyl methyl cellulose.

Herbal Preparation and Extraction

Fruits of white pepper (*Piper nigrum* L.) and long pepper (*P. longum* L.) were purchased from Anhui Taiyuan Chinese Herbal Pharmacology Co., Ltd (Voucher No., SCHM 121215). Plant samples were authenticated by Lin Dong of Pharmacognosy Department, College of Pharmacy, Ningxia Medical University. A voucher specimen was deposited in the same unit (Herbarium number, 20141220).

Residues of supercritical fluid CO₂ extract of white pepper and long pepper (20 kg) were extracted thrice for 2 hours with a 10-fold volume of ethanol (70%). Extracting solution was mixed for rotatory evaporation until the alcoholic taste was no longer detected. The yield was crude extract, which was then successively partitioned with petroleum ether and dichloromethane, ethyl acetate, butyl alcohol, and aqueous residue. These extractive fractions were then combined, evaporated to dryness, and stored at 4°C until further analyses.

Experimental Animals

Specific pathogen-free male Sprague-Dawley rats (260–320 g; license no., SCXK (NING) 2012-0001) were purchased from the Experimental Animal Center of Ningxia Medical University (Ningxia, China). Rats were individually housed in standard laboratory cages in barrier environment with moderate humidity (55% ± 5%) and constant temperature (22 ± 1°C) and were provided with food and water ad libitum under 12 h light–dark cycle prior to experiments. Experimental protocol was approved by the Ethics Committee of Ningxia Medical University, Ningxia (Ethics approval, 2015-156).

Animal pMCAO Model

Permanent middle cerebral artery occlusion (pMCAO) was performed using a previously published method with minor modification.⁷⁻⁹ After food deprivation for 12 h and water *ad libitum*, the animals were anesthetized with chloral hydrate (7%, 0.5 mL/100 g; intraperitoneal injection) and were placed in supine position (body temperature was maintained at 37°C using feedback-controlled heating pad; rats were positioned in stereotaxic frame). After performing median incision on neck skin, the right primary carotid artery (common carotid artery, external artery (ECA), and internal carotid artery (ICA)) were carefully isolated. In sham-operated control rats, right ECA was ligated; a 4-0 monofilament nylon thread (A4-2026; Sunbio Biotech, China) with rounded tip coated with poly-L-lysine was inserted from ECA into ICA up to 5–10 mm. In the remaining rats, right middle cerebral artery (MCA) was occluded with rounded tip coated with poly-L-lysine of monofilament nylon thread (A4-2026), which was inserted from ECA into ICA up to a distance of 18–20 mm. Nylon thread was cut off from and outside the blood vessels. Before the rats wake up, body temperature was maintained at normal limits (37 ± 1°C) using a heating pad.

Experimental Groups

Piper nigrum and *P. longum* samples weighed 24 g, and DF yield was 3.95%. Normal human daily dose of DF measures ($24 \times 3.95\%$) g/60 kg body weight. According to the formula $d_{\text{rat}} = d_{\text{human}} \times (6 \text{ to } 7)$, normal dose of DF for mice should be 94.80-101.06 mg/kg/day. In the present study, we selected 200 and 100 mg/kg/day as high and low dosages for the rats, respectively. To investigate neuroprotective effects of DF, we used rat pMCAO models. All rats were randomly divided into four groups, namely, the sham group, model group, and DF treatment groups. DF doses of 100 and 200 mg/kg body weight, respectively, were dissolved in 0.5% dimethyl sulfoxide/0.5% sodium carboxyl methyl cellulose (1 mL/100 g). All rats were intragastrically administered with the medicine every 6 h one day after inducing ischemia. Intragastric administration continued for 14 days.

Neurological Evaluation

In a blinded fashion, the animals were evaluated for neurological deficit score using a 6-point scale as follows: 0 = no neurological deficits, 1 = failure to extend left forepaw fully, 2 = circling to the left, 3 = paresis to the left, 4 = no spontaneous walking, and 5 = death.¹⁰ In sham-operated controls, all rats incurred 0 scores in neurological examinations. In the remaining rats, neurological examinations yielded a score of 2.

Body Weight

At 3, 6, 9, 12, and 14 days after ischemia, body weights of all rats were analyzed by animal electronic balance (Beijing Xihuayuan Technology Co., Ltd., China).

Postural Reflex

Postural reflex is a test that is sensitive to cortical and striatal lesions.¹⁰ Each rat was suspended by the tail 1 m above a table top. The animal was slowly lowered toward the table, and its posture was observed. Normal rats extended both forelimbs toward the table. This behavior received a score of 0. A score of 1 was given when the rats flexed one or both forelimbs. This animal was then given the lateral push test. This test involved placing the rat on a sheet of plastic-coated paper and applying lateral pressure behind the shoulders in the left and right directions. When the rat failed to resist the force equally in both directions, it received a score of 2. A score of 3 were given to rats circling to the left.¹¹ At 3, 6, 9, 12, and 14 days after ischemia, all rats were analyzed for postural reflex.

Body Sway

Rats were suspended by the tail 1 m above a ground top at 3, 6, 9, 12, and 14 days after ischemia, and their posture was observed. The 0-2 grade behavioral evaluation

protocol was as follows: 0, the rat symmetrically sways to left and right; 1, the rat unsymmetrically sways to the left and right (body sway < 30 degree); 2, the rat unsymmetrically sways to the left and right (body sway > 30 degree).

Balance Beam

Animals were trained to cross a 2 cm-wide \times 120 cm-long beam elevated 80 cm above the floor. A black tube placed at the far end of the beam served as a goal box (20 \times 20 \times 20 cm). Foot slips and falls were counted as faults, and the rats were given a behavioral score.¹² The 0-6 grade behavioral evaluation protocol was as follows: 0, the rat fell down upon standing on the beam; 1, the rat can stand on the beam but cannot walk further; 2, the rat fell down while walking along the beam; 3, the rat can walk along the beam but slipped in > 50% of steps; 4, the rat can walk along the beam but slipped in < 50% of steps; 5, the rat can walk on the beam but slipped after several steps; 6, the rat can walk along the beam successfully with no faults. Animals were pre-trained for 7 days and then given three trials as a baseline. At 3, 6, 9, 12, and 14 days after ischemia, the animals underwent four trials, and the number of foot faults per trial was averaged.

Grip Strength Test

Grip strength test evaluates muscle strength and neuromuscular integration relating to the grasping reflex in the forepaws.¹³ At 3, 6, 9, 12, and 14 days after ischemia, all rats were tested using a YLS-12A grip-strength-meter (Beijing Zhongshi Dichaung Technology Development Co., Ltd., China). Animals that maintained tail gripped with their forelimbs on a grid (10 cm \times 10 cm) were linked to a high-precision force sensor. This apparatus automatically records the highest pull force. The mean of all three readings was computed and used for statistical analyses.

2,3,5-Triphenyltetrazolium Chloride Staining and Evaluation of Infarct Volume

Fourteen days after ischemia, rats were deeply anesthetized by intraperitoneal injection of 10% chloral hydrate and then sacrificed. Brain tissue was removed and sectioned into six 2-mm slices quickly using a rat brain matrix (Muromachi Kikai Co., Ltd. Tokyo, Japan). Slices were placed in 2% 2,3,5-triphenyltetrazolium chloride solution for 30 minutes at 37°C. The Image J software was used for evaluation of the infarct area.

Histopathology and Immunohistochemistry

Fourteen days after ischemia, rats were anesthetized with pentobarbital chloral hydrate and perfused with 4% paraformaldehyde in 0.1 mol/L phosphate-buffered saline. Removed brains were kept in 4% paraformaldehyde for 12 h and immersed in 30% sucrose for 3-4 days

at 4°C. The brains were embedded in Wuhan Myhalic Biotechnology Co., Ltd. (Wuhan, China) and sectioned on a cryostat (4–5 μm thick). Hematoxylin and eosin (HE) staining and Nissl staining were used for histological examination. Immunohistochemistry was performed using the Histostain-Plus Bulk kit (postsynaptic density protein 95 (PSD-95), synapsin-I (syn-I), and α -synuclein (α -syn) (all Abcam)).

Western Blotting

Fourteen days after ischemia, all rats were euthanized; cerebral cortical and hippocampal tissues were quickly isolated, immediately frozen, and stored at -80°C . Cerebral cortex proteins were extracted by lysis buffer (Vazyme, China). Protein quantity was measured using BCA (Beyotime, China) assay. Equal amounts of protein samples were separated by sodium dodecyl sulfate polyacrylamide gel (PSD-95, Ca^{2+} /calmodulin (CaM)-dependent protein kinase II (CaMK II), phosphorylated CaMK II (p-CaMK II), CaM, *N*-methyl *D*-aspartate receptor (NMDAR) subtype 2B (NR2B) (all 1:1000; Abcam), and β -actin (1:1000; CST)) and electrophoresis and then transferred onto polyvinylidene difluoride membranes. After blocking with 5% nonfat milk for 1 hour at room temperature, the polyvinylidene difluoride membranes were incubated with primary antibodies at 4°C overnight and subsequently with horseradish peroxidase-conjugated secondary antibodies at room temperature for 1 hour. Protein bands were detected using enhanced chemiluminescence reagents. Chemiluminescent signals were detected and analyzed using the ChemiDoc XRS imaging system (Bio-Rad).

UPLC-Q-TOF/MS Analysis

DF were identified by UPLC-Q-TOF/MS analysis which was carried out on an Agilent 1290 UPLC system coupled to 6545 Q-TOF LC/MS system (Agilent Corp). Chromatographic analysis was performed with an Agilent Eclipse plus C18 reversed-phase LC column (2.1 \times 50 mm i.d.; 1.8 μm , Agilent) at a column temperature of 30°C. The mobile phase consisted of aqueous solution (solvent A) and methanol (solvent B) with a flow rate of 0.2 mL/min. The gradient elution program was

optimized for improved separation. The conditions were as follows: 0-15.0 minutes (60%-60% B), 15.0-18.0 minutes (60%-90% B), and 18.0-22.0 minutes (90%-60% B). Sample injection volume totaled 1 μL . Electrospray ionization source parameters included the following: drying gas (N_2) flow rate and temperature, 8.0 L/min and 320°C, respectively; nebulizer, 35 psig; capillary voltage measuring 3500 and 4000 V in the positive ion mode. Fragmentor voltages reached 150 and 175 V in the positive ion mode.

Statistical Analysis

Data are presented as mean values \pm standard deviation (SD). Statistical analysis was conducted using one-way ANOVA, followed by Dunnett's test using SPSS Version 19.0. Differences with $P < .05$ were considered statistically significant.

Results

Body Weight

A significant increase in body weight was observed in pMCAO control (model group) rats ($P < .01$) compared with the sham rats (Table 1). Compared with the model group, a significant increase in the body weight was observed in the DF (200 mg/kg)-treated groups ($P < .01$) at 6, 9, 12, and 14 days.

Postural Reflex

Postural reflex scores in pMCAO control (model group) rats ($P < .01$) significantly reduced compared with those of the sham rats (Table 2). A significant reduction in postural reflex score was observed in the 100 mg/kg DF-treated group ($P < .05$) at 6, 9, and 12 days and 200 mg/kg DF-treated groups ($P < .01$) at 9, 12, and 14 days.

Body Sway

Compared with the sham group, body sway at 3 days to 14 days showed no significant increase in the pMCAO control group ($P < .01$) (Table 3). Compared with the model group, a significant reduction was observed in the 100 mg/kg DF-treated group at 3, 6, 9, and 14 days ($P < .05$). At the same time, pMCAO rats pretreated with combination

Table 1. Effects of DF on body weight in pMCAO model rats

Groups	Evaluation time (days)				
	3	6	9	12	14
Sham	266.77 \pm 17.12	293.92 \pm 28.22	303.00 \pm 36.95	318.92 \pm 23.87	331.54 \pm 20.52
Model	221.45 \pm 14.81 ^{##}	195.82 \pm 16.36 ^{##}	185.55 \pm 19.26 ^{##}	191.64 \pm 20.74 ^{##}	187.91 \pm 24.72 ^{##}
DF 100 mg/kg	230.78 \pm 12.25	217.00 \pm 18.08	219.44 \pm 32.22	226.11 \pm 38.30	233.00 \pm 42.58
DF 200 mg/kg	240.33 \pm 22.46	265.44 \pm 22.25 ^{**}	286.00 \pm 20.48 ^{**}	306.56 \pm 26.73 ^{**}	289.22 \pm 23.76 ^{**}

Results are expressed as mean \pm SD.

^{##} $P < 0.01$, vs. sham group; ^{**} $P < 0.01$, vs. model group (N = 9–13).

Table 2. Effects of DF on postural reflex in pMCAO model rats

Groups	Evaluation time (days)				
	3	6	9	12	14
Sham	0.00 ± 0.00	0.00 ± 0.00	0.00 ± 0.00	0.00 ± 0.00	0.00 ± 0.00
Model	1.81 ± 0.40 ^{###}	1.82 ± 0.40 ^{###}	2.00 ± 0.00 ^{###}	1.91 ± 0.30 ^{###}	1.91 ± 0.30 ^{###}
DF 100 mg/kg	1.33 ± 0.87	0.89 ± 0.60*	0.78 ± 0.44**	0.56 ± 0.53**	0.89 ± 0.93
DF 200 mg/kg	1.89 ± 0.33	1.56 ± 0.53	0.67 ± 0.50**	0.33 ± 0.50**	0.56 ± 0.53**

Results are expressed as mean ± SD.

^{###} $P < 0.01$, vs. sham group; * $P < 0.05$, ** $P < 0.01$, vs. model group (N = 9~13).

Table 3. Effects of DF on body sway in pMCAO model rats

Groups	Evaluation time (days)				
	3	6	9	12	14
Sham	0.00 ± 0.00	0.00 ± 0.00	0.00 ± 0.00	0.00 ± 0.00	0.00 ± 0.00
Model	1.82 ± 0.60 ^{###}	2.00 ± 0.00 ^{###}	2.00 ± 0.00 ^{###}	1.64 ± 0.67 ^{###}	2.00 ± 0.00 ^{###}
DF 100 mg/kg	0.44 ± 0.53**	0.56 ± 0.88*	0.89 ± 0.78*	0.89 ± 0.93	0.89 ± 0.78*
DF 200 mg/kg	0.56 ± 0.53**	0.78 ± 0.97	0.11 ± 0.33**	0.22 ± 0.44**	0.22 ± 0.44**

Results are expressed as mean ± SD.

^{###} $P < 0.01$, vs. sham group; * $P < 0.05$, ** $P < 0.01$, vs. model group (N = 9~13).

of DF 200 mg/kg presented significantly ($P < .05$) reduced body sway scores compared with the pMCAO control group (Table 3).

Balance Beam

Effects of DF treatment were observed in groups walking on balance beam at 2 weeks. Although all groups showed higher average foot faults than the sham group, only the DF 200 mg/kg group significantly differed from the model group at each time point ($P < .01$, Table 4).

Grip Strength Test

After pMCAO modeling, grip strength test scores of pMCAO control rats ($P < .01$) was significantly reduced compared with those of the sham rats (Table 5). Interestingly, only pMCAO rats pretreated with combination of DF 200 mg/kg exhibited significantly ($P < .01$) improved grip strength test scores compared with the pMCAO model group (Table 5).

2,3,5-Triphenyltetrazolium Chloride Staining and Evaluation of Infarct Volume

At 14 days after pMCAO, rats in the sham group did not show any evidence of cerebral infarction. Compared with the group of Model, DF_{100mg/kg} and DF_{200mg/kg} rats, there were different degrees of infarction (Fig 1A). The infarct volume was significantly reduced after DF treatment ($P < .05$; Fig 1B).

Histopathology and Immunohistochemistry

As the improved functional outcome will result from reduced brain damage, we tested the effects of DF on brain infarct volume by performing HE staining and Nissl staining at 14 days after pMCAO. Injury was mostly notable in subcortical regions, mainly the striatum, and in areas of the cerebral cortex (Figs. 2 and 3). No damage was observed in sham-operated rats. Nucleolus was prominent, and nuclear membrane was relatively intact. Neurons of those followed an ordered arrangement, and glial cells and capillary

Table 4. Effects of DF on walking on balance beam in pMCAO model rats

Groups	Evaluation time (days)				
	3	6	9	12	14
Sham	5.69 ± 0.48	5.62 ± 0.51	5.62 ± 0.51	5.92 ± 0.28	5.92 ± 0.28
Model	0.45 ± 0.52 ^{###}	1.18 ± 0.40 ^{###}	1.18 ± 0.87 ^{###}	1.45 ± 0.93 ^{###}	2.09 ± 0.94 ^{###}
DF 100 mg/kg	1.56 ± 1.42	2.78 ± 1.09*	3.33 ± 1.66	4.00 ± 1.73*	4.33 ± 1.80
DF 200 mg/kg	2.89 ± 1.45**	4.33 ± 1.41**	4.44 ± 1.24**	5.33 ± 0.71**	4.78 ± 1.30**

Results are expressed as mean ± SD.

^{###} $P < 0.01$, vs. sham group; * $P < 0.05$, ** $P < 0.01$, vs. model group (N = 9~13).

Table 5. Effects of DF on grip strength test in pMCAO model rats

Groups	Evaluation time (days)				
	3	6	9	12	14
Sham	936.85 ± 109.99	1000.00 ± 142.07	1129.08 ± 97.51	1129.08 ± 168.59	1200.46 ± 115.27
Model	737.18 ± 147.21 ^{##}	786.00 ± 116.05 ^{##}	871.73 ± 161.69 ^{##}	803.36 ± 165.26 ^{##}	862.45 ± 164.52 ^{##}
DF _{100 mg/kg}	868.44 ± 175.36	974.22 ± 116.73 ^{**}	970.11 ± 93.45	1028.78 ± 36.24	1065.44 ± 84.38
DF _{200 mg/kg}	913.89 ± 123.06 ^{**}	1064.78 ± 139.51 ^{**}	1122.89 ± 133.55 ^{**}	1188.11 ± 99.82 ^{**}	1137.56 ± 144.13 [*]

Results are expressed as mean ± SD.

^{##} $P < 0.01$, vs. sham group; ^{*} $P < 0.05$, ^{**} $P < 0.01$, vs. model group (N = 9~13).

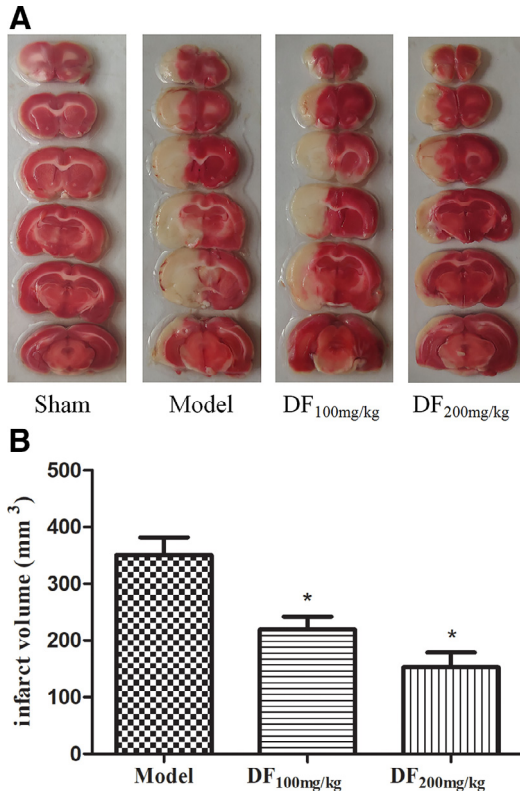


Figure 1. Changes of infarct volume after DF treatment. (A) TTC staining photograph in Sham, Model, and treated with DF groups. (B) Results from the measurement of infarct volume in the ischemia and treated with DG groups ($*P < .05$).

DF, dichloromethane fraction; TTC, triphenyltetrazolium chloride.

morphogenesis were normal. After pMCAO modeling, edema of the neuropile was observed in the ischemic area, and most neurons in the damage area appeared shrunken with eosinophilic cytoplasm and triangulated pyknotic nuclei. The infarct core was surrounded with ischemic injured neurons. After DF treatment, cortex regions of infarct core in the ischemic brain tissue significantly improved. Specifically, the treatment of 200 mg/kg DF resulted in the most remarkable improvement in ischemic injury when compared with the model group (Fig. 2). As expected, pMCAO surgery significantly reduced the

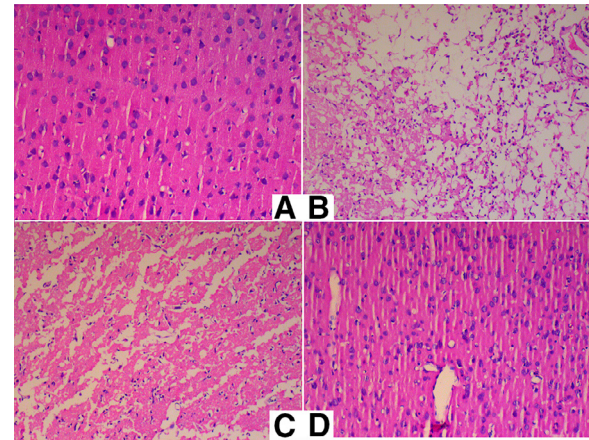


Figure 2. Effects of DF on HE staining of cerebral ischemia in rats. Sham group (A), model group (B), DF_{100 mg/kg} group (C), and DF_{200 mg/kg} group (D).

DF, dichloromethane fraction.

number and size of neurons smaller and caused their irregular arrangement in brain regions compared with that of sham group (Fig. 3). Treatment with DF significantly increased neuronal density and decreased the number of shrunken neuronal cell bodies compared with treatment of the model group, coinciding with the observations in the preceding neurobehavioral tests.

DF was activated in cerebral ischemia area. Expression levels of PSD-95, syn-I, and α -syn serve as important indicators of DF activation. PSD-95, syn-I, and α -syn expressions in cerebral ischemia area were detected by immunohistochemistry, and positive-cell-integrated option density was counted (Fig. 4B). Compared with the sham group, no significant change was observed in immunostaining of PSD-95, syn-I, and α -syn in ischemic brain tissue of model rats. PSD-95 values were increased significantly by DF 200 mg/kg compared with the model group ((0.0775 ± 0.0189), ($P < .01$)). Fig. 4 shows that syn-I level in model rats increased significantly, whereas this increase was reduced markedly in DF (100 and 200 mg/kg)-treated rats (both $P < .01$). However, α -syn levels reduced significantly in DF-treated group (both $P < .01$) compared with the model group (0.1101 ± 0.0124). Higher concentration of DF was predicted to feature more significant inhibition.

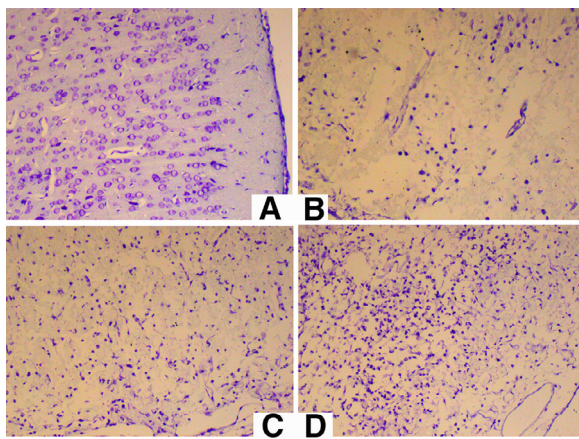


Figure 3. Effects of DF on Nissl staining of cerebral ischemia in rats. Sham group (A), model group (B), DF₁₀₀ mg/kg group (C), and DF₂₀₀ mg/kg group (D).
DF, dichloromethane fraction.

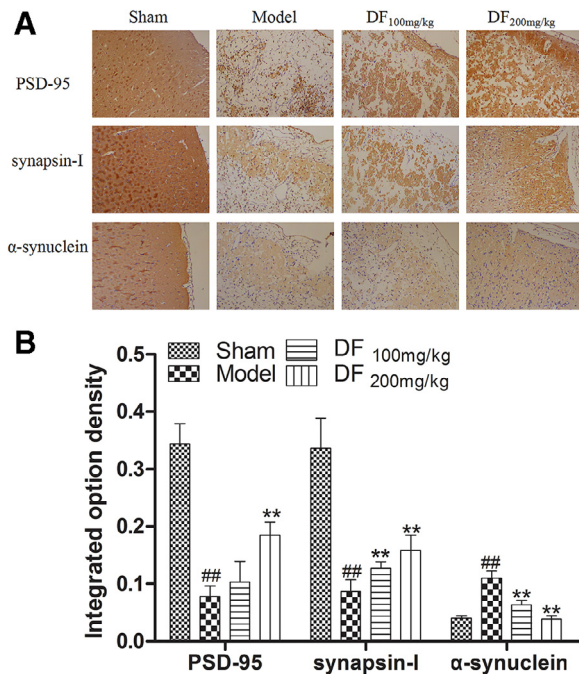


Figure 4. PSD-95, syn-I, and α -syn were detected by immunohistochemistry. (A) Postsynaptic density -95, syn-I, and α -syn-labeled cells in ischemic area of the brain after 14 days of pMCAO. (B) Counting of positive-cell-integrated option density. Scale was 50 mm at 400 magnification under light microscopy. Compared with the sham group: * $P < .05$, ** $P < .01$. Compared with the model group: * $P < .05$, ** $P < .01$.
pMCAO, permanent middle cerebral artery occlusion; PSD, postsynaptic density protein.

Western Blotting

Following histopathological and immunohistochemistry analyses, Western blot analyses revealed detectable protein expression levels of PSD-95, p-CaMK II, CaMK II, CaM, NR2B, and β -actin in the sham, model, and DF-treated groups. As shown in Fig. 5A, compared with the

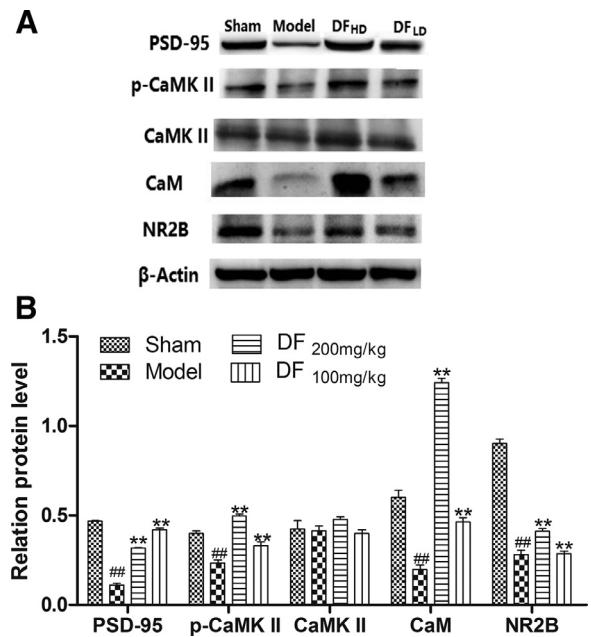


Figure 5. Effects of PSD-95, p-CaMK II, CaMK II, CaM, and NR2B expression in the cortex after pMCAO. β -Actin bands served as internal cytoplasmic controls. Data are expressed as means \pm SD; $n = 4$. Compared with the sham group: # $P < .05$, ## $P < .01$. Compared with the model group: * $P < .05$, ** $P < .01$.
pMCAO, permanent middle cerebral artery occlusion.

sham group, the model group exhibited a noticeable reduction in PSD-95, p-CaMK II, CaM, and NR2B compared with the model group, whereas DF increased PSD-95, p-CaMK II, CaM, and NR2B ($P < .05$). No differences were observed among groups regarding CaMK II immunoblotting as shown in Fig. 5B. Therefore, PSD-95, p-CaMK II, CaM, and NR2B may represent neurorestorative response in the ischemic brain of DF-treated mice.

Identification of Compounds From DF by UHPLC-Q-TOF-MS

To identify the major components of DF, we analyzed DF by UHPLC-Q-TOF-MS. Based on retention times, eight major components in the UHPLC-Q-TOF-MS fingerprint of DF were identified (Area %): piperoglin (2.25%), pipericyclobutanamide G (0.76%), hinokinin (3.22%), piperine (65.68%), N-(5,6,7,8-tetrahydronaphthalen-2-yl) acetamide (2.23%), piperonaline (1.63%), E-4(15)-eudesmene-1 β ,6 α -diol (1.82%), and piperolein-B (1.06%) (Fig. 6).

Discussion

The present study demonstrates the dose-dependent neuroprotective effects of DF at 100 and 200 mg/kg orally administered in the pMCAO model of stroke in rats. Motor dysfunction is the most prominent clinical stroke deficit. In this study, we also observed an increase turning behavior in pMCAO rats. Neuroprotective effects were evident from significant improvements in body weight,

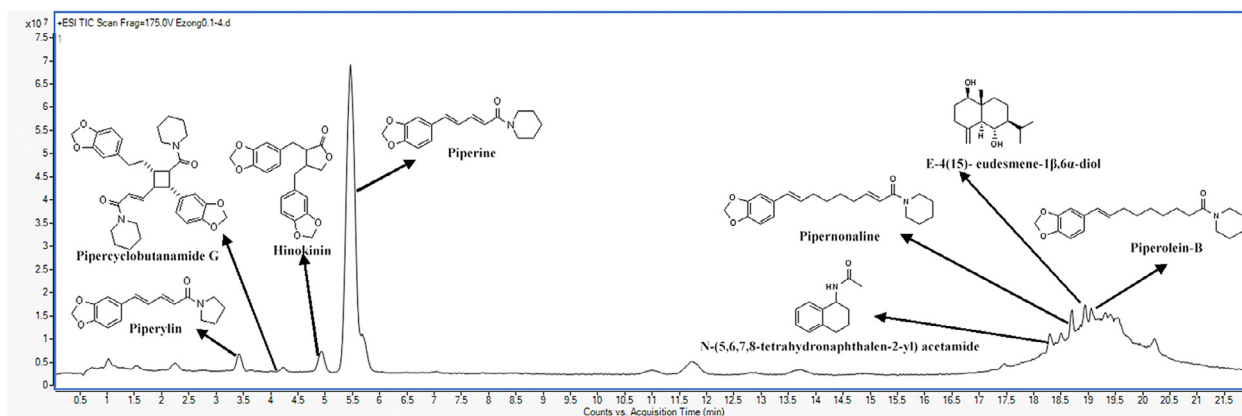


Figure 6. UPLC chromatograms of DF from *Piper nigrum* L. and *Piper longum* L. DF, dichloromethane fraction; UPLC, ultrahigh-performance liquid chromatography.

neurological dysfunction, postural reflex, body sway, beam balancing, and grip strength. Motor dysfunction results from damages of the motor cortex and pyramidal tracts, which lie within the MCA territory, leading to unrecoverable loss of synaptic activity in the motor cortex and subsequent blockade of electrical activity in subcortical regions.^{14,15}

Histological findings yielded similar results. Ischemia areas exhibited cell swelling, nuclear shrinkage, and degeneration in HE staining. Nissl staining is a widely used method for studying the morphology and pathology of neural tissues. The Nissl bodies engaged in active protein synthesis include neurotransmitter synthesis-related enzymes and peptides.¹⁶ Nissl staining with neuron specificity showed notable nuclear shrinkage, thinning, and necrosis. As expected, pMCAO surgery significantly increased cell nuclear shrinkage and degeneration (HE staining) and reduced the number and size of neurons (Nissl staining) in cerebral cortex regions compared with those of the sham group. DF treatment with doses of 100 and 200 mg/kg significantly reduced cell nuclear shrinkage, inhibited neuronal degeneration, and increased Nissl body density and decreased the number of shrunken neuronal cell bodies in all indicated regions of the cerebral cortex.

Synapses refer to the critical junctions between neurons and where significant signaling and communication between neural cells occur. PSD-95 protein is the major scaffold protein of dendritic spines within PSD, and it facilitates anchorage of membrane receptors in spines, controls the partnership between neurotransmitters and receptors, and finally determines synaptic responses.^{17,18} The study showed that PSD-95 significantly influences neuronal survival and synaptic function on cerebral ischemia in late stage.¹⁹ Syn-I is assumed to be involved in regulating neurotransmitter release and in synapse formation; ischemic insults possibly modify presynaptic proteins.²⁰ α -Syn is a synaptic protein involved in synaptic plasticity and neurodegeneration and a highly conserved 140-amino acid protein that is predominantly

expressed in neurons; it is predominantly expressed in the cerebral cortex and hippocampus.^{21,22} In our present study, PSD-95 and syn-I significantly increased, whereas α -syn decreased after onset of cerebral ischemia. These results revealed that nerve damage on synaptic occurred following focal cerebral ischemic injury in rats. DF treatment at a dose of 100 mg/kg significantly inhibited increases in α -syn and promoted production of syn-I in brain tissues of rats after pMCAO injury. DF treatment at a dose of 200 mg/kg significantly increased PSD-95 and syn-I, whereas α -syn significantly decreased in cerebral cortex of rats after pMCAO injury. Thus, we presume that DF plays a fundamental role of protecting against nerve damage in focal cerebral ischemia through amelioration of protection of synaptic neurons.

Ischemic stroke leads to energy metabolism dysfunction, massive influx of calcium (Ca^{2+}), excessive glutamate release, and overactivation of NMDAR, resulting in neuronal damage and death.²³ Neuronal damage or demise is largely due to sustained activation of NMDARs for glutamate, with a consequent increase in intracellular Ca^{2+} concentration and activation of calcium-dependent mechanisms.²⁴ Effects of Ca^{2+} on cellular functions may be mediated by Ca^{2+} -binding proteins and CaM.²⁵ CaMK II is a potential Ca^{2+} target; it is concentrated in PSD in the brain, can phosphorylate a large number of proteins, and plays an important role in neurotransmitter exocytosis, with neurons exciting regulation of long-term potentiation.²⁶⁻²⁸ At the same time, p-CaMK II can regulate the T-type calcium channel, which is involved with regulation of intracellular calcium ion-activating CaM.²⁸ NMDARs constitute the major subtype of glutamate receptors and normally participate in linking multiple intracellular catabolic processes responsible for irreversible neuronal death.²⁹ NR2B-containing NMDAR are considered the main types of functional NMDAR channels in central nervous system neurons.³⁰ The present results showed that expression levels of proteins PSD-95, p-CaMK II, CaM, and NR2B decreased in the model group. By contrast, DF treatment significantly increased levels of PSD-95, p-CaMK II, CaM, and NR2B in the cortex ($P < .05$;

$P < .01$). Expression levels of CaMK II showed no notable change in each group. These results suggest that excitement of PSD-95, p-CaMK II, CaM, and NR2B proteins may be involved in inhibition of excessive glutamate release, massive influx of Ca^{2+} , and overactivation of NMDAR in pMCAO. Thus, we presume that DF plays an important role in focal cerebral ischemia therapy.

Meanwhile, we used UHPLC-Q-TOF-MS to determine the major component of DF, whose primary component is piperine (65.68%, Area %). Piperine was established as an antioxidant, anti-inflammatory, cognitive enhancer and protector of neurons.³¹⁻³³ Our previous research also showed that piperine could be used to treat permanent focal cerebral ischemia injury through antioxidant activity.³⁴ Thus, piperine bears importance in treating brain damage of rats with permanent focal cerebral ischemia injury and features potential use in development of new drugs. Next, we will use piperine to do further experiments to test our conjecture.

References

- Global, regional, and national disability-adjusted life-years (DALYs) for 333 diseases and injuries and healthy life expectancy (HALE) for 195 countries and territories, 1990-2016: a systematic analysis for the Global Burden of Disease Study 2016. *Lancet* 2017;390:1260-1344.
- Global, regional, and national age-sex specific mortality for 264 causes of death, 1980-2016: a systematic analysis for the Global Burden of Disease Study 2016. *Lancet* 2017;390:1151-1210.
- Kaminski HJ. An introduction to molecular neurobiology. *Neurology* 1992;42:2061.
- Kim HG, Han EH, Jang WS, et al. Piperine inhibits PMA-induced cyclooxygenase-2 expression through down regulating NF-kappaB, C/EBP and AP-1 signaling pathways in murine macrophages. *Food Chem Toxicol* 2012;50:2342-2348.
- Son DJ, Kim SY, Han SS, et al. Piperlongumine inhibits atherosclerotic plaque formation and vascular smooth muscle cell proliferation by suppressing PDGF receptor signaling. *Biochem Biophys Res Commun* 2012;427:349-354.
- Zhang Y, Wang X, Ma L, et al. Anti-inflammatory, antinociceptive activity of an essential oil recipe consisting of the supercritical fluid CO₂ extract of white pepper, long pepper, cinnamon, saffron and myrrh in vivo. *J Oleo Sci* 2014;63:1251-1260.
- Koizumi JI, Yoshida Y, Nakazawa T, et al. Experimental studies of ischemic brain edema: 1. A new experimental model of cerebral embolism in rats in which recirculation can be introduced in the ischemic area. *Jpn J Stroke* 1986;8:1-8.
- Luo Y, Yang YP, Liu J, et al. Neuroprotective effects of madecassoside against focal cerebral ischemia reperfusion injury in rats. *Brain Res* 2014;1565:37-47.
- Nagasawa H, Kogure K. Correlation between cerebral blood flow and histologic changes in a new rat model of middle cerebral artery occlusion. *Stroke* 1989;20:1037-1043.
- Bederson JB, Pitts LH, Tsuji M, et al. Rat middle cerebral artery occlusion: evaluation of the model and development of a neurologic examination. *Stroke* 1986;17:472.
- Alexis NE, Back T, Zhao W, et al. Neurobehavioral consequences of induced spreading depression following photothrombotic middle cerebral artery occlusion. *Brain Res* 1996;706:273-282.
- Li L, Li Y, Ji X, et al. The effects of retinoic acid on the expression of neurogranin after experimental cerebral ischemia. *Brain Res* 2008;1226:234.
- Ferrara A, El BS, Seyen S, et al. The usefulness of operant conditioning procedures to assess long-lasting deficits following transient focal ischemia in mice. *Behav Brain Res* 2009;205:525-534.
- Bolay H, Dalkara T. Mechanisms of motor dysfunction after transient MCA occlusion: persistent transmission failure in cortical synapses is a major determinant. In: *IEEE First AESS European Conference on Satellite Telecommunications*; 1998. p. 1-5.
- Gupta S, Gupta YK. Combination of Zizyphus jujuba and silymarin showed better neuroprotective effect as compared to single agent in MCAO-induced focal cerebral ischemia in rats. *J Ethnopharmacol* 2016;197:118-127.
- Kā DRA, Wittmann G, Liposits Z, et al. Improved method for combination of immunocytochemistry and Nissl staining. *J Neurosci Meth* 2009;184:115-118.
- Savioz A, Leuba G, Vallet PG. A framework to understand the variations of PSD-95 expression in brain aging and in Alzheimer's disease. *Ageing Res Rev* 2014;18:86.
- Okabe S. Molecular anatomy of the postsynaptic density. *Mol Cell Neurosci* 2007;34:503-518.
- Martone ME, Jones YZ, Young SJ, et al. Modification of postsynaptic densities after transient cerebral ischemia: a quantitative and three-dimensional ultrastructural study. *J Neurosci* 1999;19:1988-1997.
- Jung YJ, Park SJ, Park JS, et al. Glucose/oxygen deprivation induces the alteration of synapsin I and phosphosynapsin. *Brain Res* 2004;996:47-54.
- Dufty BM, Warner LR, Hou ST, et al. Calpain-cleavage of α -synuclein: connecting proteolytic processing to disease-linked aggregation. *Am J Pathol* 2007;170:1725-1738.
- Sato K, Yamashita T, Kurata T, et al. Telmisartan reduces progressive oxidative stress and phosphorylated α -synuclein accumulation in stroke-resistant spontaneously hypertensive rats after transient middle cerebral artery occlusion. *J Stroke Cerebrovasc* 2014;23:1554-1563.
- Chen B, Wang G, Li W, et al. Memantine attenuates cell apoptosis by suppressing the calpain-caspase-3 pathway in an experimental model of ischemic stroke. *Exp Cell Res* 2017;351:163-172.
- Curcio M, Salazar IL, Mele M, et al. Calpains and neuronal damage in the ischemic brain: the Swiss knife in synaptic injury. *Prog Neurobiol* 2016;143:1-35.
- Jusuf AA, Susilowati R, Sakagami H, et al. Expression of Ca²⁺/calmodulin-dependent protein kinase (CaMK) I β 2 in developing rat CNS. *Neuroscience* 2002;109:407.
- Chen HX, Otmakhov N, Strack S, et al. Is persistent activity of calcium/calmodulin-dependent kinase required for the maintenance of LTP? *J Neurophysiol* 2001;85:1368-1376.
- Easley CA, Faison MO, Kirsch TL, et al. Laminin activates CaMK-II to stabilize nascent embryonic axons. *Brain Res* 2006;1092:59-68.
- Wen X, Lai X, Li X, et al. The effects of ropivacaine hydrochloride on the expression of CaMK II mRNA in the dorsal root ganglion neurons. *Biomed Pharmacother* 2016;84:2014-2019.
- Tu W, Xu X, Peng L, et al. DAPK1 interaction with NMDA receptor NR2B subunits mediates brain damage in stroke. *Cell* 2010;140:222-234.

30. Madden DR. Ion channel structure: the structure and function of glutamate receptor ion channels. *Nat Rev Neurosci* 2002;3:91-101.
31. Singh P, Singh IN, Mondal SC, et al. Platelet-activating factor (PAF)-antagonists of natural origin. *Fitoterapia* 2013;84:180.
32. Hu D, Wang Y, Chen Z, et al. The protective effect of piperine on dextran sulfate sodium induced inflammatory bowel disease and its relation with pregnane X receptor activation. *J Ethnopharmacol* 2015;169:109-123.
33. Wang H, Liu J, Gao G, et al. Protection effect of piperine and piperlonguminine from *Piper longum* L. alkaloids against rotenone-induced neuronal injury. *Brain Res* 2016;1639:214.
34. Wang B, Zhang Y, Huang J, et al. Anti-inflammatory activity and chemical composition of dichloromethane extract from *Piper nigrum* and *P. longum* on permanent focal cerebral ischemia injury in rats. *Rev Bras Farmacogn* 2017;3:369-374.